

Solvent control of crack dynamics in a reversible hydrogel

Tristan Baumberger,* Christiane Caroli, and David Martina

INSP, Université Pierre et Marie Curie-Paris 6,

Université Denis Diderot-Paris 7, CNRS, UMR 7588 Campus Boucicaut,

140 rue de Lourmel, 75015 Paris, France.

(Dated: October 5, 2018)

The resistance to fracture of reversible biopolymer hydrogels is an important control factor of the cutting/slicing and eating characteristics of food gels¹. It is also critical for their utilization in tissue engineering, for which mechanical protection of encapsulated components is needed^{2,3}. Its dependence on loading rate⁴ and, recently, on the density and strength of cross-links³ has been investigated. But no attention was paid so far to solvent nor to environment effects. Here we report a systematic study of crack dynamics in gels of gelatin in water/glycerol mixtures. We show on this model system that: (i) increasing solvent viscosity slows down cracks; (ii) soaking with solvent increases markedly gel fragility; (iii) tuning the viscosity of the (miscible) environmental liquid affects crack propagation via diffusive invasion of the crack tip vicinity. The results point toward the fact that fracture occurs by viscoplastic chain pull-out. This mechanism, as well as the related phenomenology, should be common to all reversibly cross-linked (physical) gels.

Gelatin gels are constituted of denatured (coil) collagen chains, held together by cross-links made of segments of three-stranded helices stabilized by hydrogen bonds⁵. This network, swollen by the aqueous solvent, which controls its (undrained) bulk modulus, is responsible for the finite shear modulus μ , of order a few kPa. Hence, hydrogels can be considered incompressible. One estimates average mesh sizes $\xi \sim (kT/\mu)^{1/3}$ of order 10 nm, i.e. coil segments involving a few 100 units (residues)⁶. Moreover, in the presence of pressure gradients, the solvent diffuses through the network. This poroelastic behaviour^{7,8} controls e.g. slow solvent draining in or out of the gel under applied stresses.

They are *thermoreversible*, i.e., in contrast with chemical, covalently cross-linked gels, their network "melts" close above room temperature. This behavior, assignable to their small cross-link binding energy, leads to the well studied⁵ slow aging (strengthening) of μ , and to their noticeable creep under moderate stresses⁹. When stretched at constant strain rate, gelatin gels ultimately fail at a strain ~ 1 which, though rather poorly reproducible, is clearly rate-dependent⁴. In order to get insight into the nature of the dissipative processes at play, one needs to investigate the propagation of cracks independently from their (stochastic) nucleation¹⁰. Here we study the fracture energy $\mathcal{G}(V)$ needed to propagate a crack at constant velocity V in notched long thin plates (see Fig. 1) of gels differing by the glycerol content of their aqueous solvent.

As seen on Figure 2(a), \mathcal{G} is very strongly velocity and solvent-dependent. Our gels are velocity toughening: at fixed ϕ , \mathcal{G} grows quasi-linearly over the whole investigated V -range (0.1–30 mm.s⁻¹). Linear extrapolation down to $V = 0$ yields an evaluated quasi-static toughness \mathcal{G}_0 . Within experimental accuracy, \mathcal{G}_0 is of order 2.5 J.m⁻², i.e. about 20 times larger than a gel-air surface energy, and ϕ -independent. In contrast, $\mathcal{G}(V)$ becomes noticeably steeper as ϕ increases. Plotting it versus ηV (Fig. 2(b)) captures most of this dependence. Note that the ratio $\mathcal{G}/\eta V$ is a huge *number* of order 10⁶.

This points toward the critical role of network/solvent relative motion. In particular, the impossibility for not very thin, quasi incompressible plates to accomodate fully the high local strain gradients developing in the crack tip region results in high negative pressures. So, most likely, solvent is partly drained out of this region into the bulk, leading for the chains thus exposed to air, to a solvation energy cost. We investigate this issue with the help of experiments in which a drop of the gel solvent is introduced into the already moving crack opening. Such tip wetting induces, at fixed sample stretching, a positive, V -independent velocity jump (Fig. 3). Equivalently, wetting decreases $\mathcal{G}(V)$ by a constant $\Delta\mathcal{G}_0$. For $\phi = 0$, $\Delta\mathcal{G}_0 \sim 2$ J.m⁻² is a substantial fraction of \mathcal{G}_0 .

Can one make, on the basis of these results, a plausible guess about the nature of the fracture mechanism in reversible hydrogels?

Clearly, one cannot invoke here the classical Lake-Thomas picture¹¹, which successfully accounts for rubber toughness. Indeed, in these materials, fracture occurs via chain scission: polymer segments crossing the fracture plane are stretched taut until they store an elastic energy per monomer of order the covalent binding one, $U_{chain} \sim$ a few eV. In thermoreversible gels, the corresponding force, $\sim U_{chain}/a$, is more than two orders of magnitude larger than that, $f^* \sim U_{CL}/a$, which can be sustained by the H -bond stabilized cross-links (CL). U_{CL} is the segmental unbinding energy introduced in the zipper¹² and reel-chain¹³ models of gel elasticity. This leads us to postulate that, in the highly stressed "active crack tip zone", cross-links yield, up till the stretched chains are pulled out of the matrix. The threshold stress σ^* at the onset of CL-yield can be estimated as $\sigma^* \sim f^*/\xi^2 = U_{CL}/a\xi^2$. With $a \sim 0.3$ nm, $U_{CL} \sim 10^{-1}$ eV, $\xi \sim 10$ nm, $\sigma^* \sim 500$ kPa, two orders of magnitude larger than a small strain shear modulus.

When solvent can be pumped from a wetting drop, the plastic zone deforms under this constant stress till the opening δ_c at the tip reaches the length ℓ of a fully stretched chain.

This Dugdale-like picture¹⁴ yields for the quasi-static fracture energy :

$$\mathcal{G}_0^{wet} = \sigma^* \ell \quad (1)$$

from which we get $\ell \sim 1.2 \mu\text{m}$. With an average mass $M_{res} = 80 \text{ Da}$ per residue, this yields for the gelatin molar weight the reasonable estimate: $M_{res}\ell/a \sim 320 \text{ kDa}$.

Let us turn to the V -dependence of \mathcal{G} . A finite V means a finite pull-out velocity $\dot{\delta} = \alpha V$. Determining the value and precise space variation of $\alpha = d\delta/dx$ in the active zone would demand solving for the whole stress field. Given the large value of σ^*/μ , this would raise such intricate, still unsolved issues as strain-induced helix/coil transition⁶, elastic crack blunting and strain hardening at large deformation¹⁵. Failing anything better, we take α to be an unknown geometrical factor.

We then write for the viscoplastic stress $\sigma = \sigma^* + \sigma_{vis}(V)$. The viscous stress σ_{vis} can be evaluated as resulting from hydrodynamic friction of chains of contour length ℓ pulled at velocity $\dot{\delta}$ out of “tubes” formed by the embedding network. A natural candidate for the radius of these tubes is the effective pore size ξ_{hydr} extracted from light scattering experiments¹⁶ (see Methods). So, $\sigma_{vis} \approx \alpha \eta V \ell / \xi_{hydr}^2$, and

$$\mathcal{G}(V) \approx \mathcal{G}_0 + \ell \sigma_{vis} = \mathcal{G}_0 + \alpha \left(\frac{\ell}{\xi_{hydr}} \right)^2 \eta V \quad (2)$$

So, this schematic model does account for the linear $\mathcal{G}(V)$ variation. Moreover, with $\xi_{hydr} = 2.7 \text{ nm}$, it predicts a reduced slope $d\mathcal{G}/d(\eta V) \approx 2.5 \times 10^5 \alpha$. When compared with experimental values ($\sim 10^6$) this suggests α values of order unity, possibly associated with elastic blunting¹⁵.

Beyond this, the remaining splay between the $\mathcal{G}(\eta V)$ curves (Fig. 2(b)) appears positively correlated with elastic stiffness variations: as is the case for reversible alginate gels³, “the stiffer, the tougher” — a relationship currently under more systematic investigation.

In this picture, draining at a non-wetted tip results in a capillary energy cost per chain $\Delta\mathcal{G}_0 \cdot \xi^2 \sim 1000 \text{ eV}/\text{chain}$, i.e. $\sim 10 kT$ per residue, a value which suggests that chains are extracted individually rather than as gel fibrils. The observed V -independence of $(\mathcal{G}^{dry} - \mathcal{G}^{wet})$ indicates that α , hence the geometry of the active zone, is largely unaffected by wetting.

We can now take one further step. Our scenario suggests that we should be able to tune, at fixed grips, the crack velocity by using a wetting drop with a glycerol content ϕ_{drop} , hence a viscosity, different from that of the gel solvent. We expect that, for small

enough V , the miscible wetting fluid will invade the whole active zone, bringing V to its value for a ϕ_{drop} -gel. The faster the crack, the less efficient this diffusive mixing process: the hetero-wetted $\mathcal{G}(V)$ should gradually approach that for the homo-wetted ϕ -gel. The result for cracks in a $\phi = 30\%$ gel wetted by pure water, shown on Figure 4, spectacularly confirms this expectation.

Moreover, assuming that the cross-over range (V_1, V_2) (Fig. 4) corresponds to diffusion lengths D_{eff}/V decreasing from d_{act} to ξ , we estimate for the diffusion constant of glycerol in the stretched gel $D_{eff} \sim V_2\xi \sim 2 \times 10^{-10} \text{ m}^2/\text{s}$, and for the size of the active zone in the gel matrix $d_{act} \sim \xi V_2/V_1 \sim 100 \text{ nm}$.

We conclude from this work that due to their weak binding responsible for cross-link plasticity^{3,9,13}, thermoreversible gels fracture via chain pull-out. While the fracture threshold is controlled by the cross-link yield stress, i.e. by the network only, crack dynamics is ruled by chain/solvent friction. This opens promising perspectives toward solvent control of crack dynamics in these materials, since: (i) The larger bulk solvent viscosity is, the slower cracks under a given loading, (ii) Homowetting of a crack tip speeds it up and can set subcritical precracks into motion, (iii) Heterowetting by a miscible fluid with substantial viscosity contrast leads, via diffusive “rinsing” of the active zone, to drastic effects on the propagation of slow cracks.

So, tip wetting appears as a method of local and fast control of crack dynamics in such materials. Conversely, our results call attention to the fact that characterization of gel fracture properties should be performed under realistic, e.g. physiological, environmental conditions.

METHODS

Gel sample preparation

Gels are prepared by dissolving 5 wt% gelatin powder (type A from porcine skin, Sigma) in mixtures of glycerol ($\phi = 0, 20, 30, 60 \text{ wt}\%$) in deionized water, under continuous stirring at 90° C , an unusually high temperature needed to get homogeneous pre-gel solutions at high ϕ ¹⁹. A control experiment performed with a pure water/gelatin sample prepared at 60° C resulted in differences on low strain moduli and $\mathcal{G}(V)$ slopes of, respectively, 1% and 7%,

compatible with scatters between samples prepared at 90° C, whence we conclude that our preparation method does not induce significant gelatin hydrolysis.

The solution is then poured into a mold consisting of a rectangular frame and two plates covered with Mylar[®] films. On the longest sides of the frame, the curly half-part of an adhesive Velcro[®] tape improves the gel plate grip. The mold is set at $2 \pm 0.5^\circ$ C for 15 hrs, then clamped to the mechanical testing set-up and left at room temperature ($19 \pm 1^\circ$ C) for 1 hr. The removable pieces of the mold are subsequently taken off, leaving the $300 \times 30 \times 10$ mm³ gel plate fixed to its grips. The Mylar[®] films are left in position in order to prevent solvent evaporation. They are peeled off just before performing an experiment.

Hydrogel characterization

Small strain shear moduli μ are computed from the force-elongation curves assuming incompressibility, plane stress deformation and neglecting finite-size effects. A high glycerol content significantly stiffens the gels, from $\mu = 3.5$ kPa at $\phi = 0$ to $\mu = 5.2$ kPa at $\phi = 60$ %, possibly due to ϕ -dependent solvent-chain interactions. Large deformation, non-linear curves up to stretching ratios $\lambda \simeq 1.5$ are integrated numerically to determine the elastic energy $\mathcal{F}(\lambda)$ stored in stretched plates.

The collective diffusive mode of the polymer network in the solvent^{7,8} is characterized by the diffusion coefficient D_{coll} , measured by dynamic light scattering as described elsewhere¹⁷. Solvent viscosities η range from 10^{-3} Pa.s at $\phi = 0$ to 11×10^{-3} Pa.s at $\phi = 60$ %. Accordingly, D_{coll} decreases as ϕ increases. One estimates an effective pore size as $\xi_{hydr} = \sqrt{D_{coll}\eta/\mu}$. It is found independent of ϕ within experimental accuracy : $\xi_{hydr} = 2.7 \pm 0.2$ nm.

Fracture experiments

Before stretching, a knife-cut notch is made at one edge of the plate. The grips are then pulled apart for 1 second by an amount $\Delta h = \lambda h_0$, with $h_0 = 30$ mm the height of the plate. The stiffness of the load cell is such that fracture occurs at fixed grips. A video movie of the plate is recorded at a typical 15 frame.s^{-1} rate and post-treated for tracking the crack tip position. Away from the sample edges, cracks run at a constant velocity V (see Fig. 1). Further data processing is restricted to this region. V is computed by linear regression of

the tip position. Since reversible gels creep, the investigated range is restricted to velocities large enough for the energy released by stress relaxation of the gel to be negligible compared with that released by crack propagation.

The energy released by unit area of crack advance is computed from the elastic energy of the uncracked plate $\mathcal{F}(\lambda)$ as¹⁸ : $\mathcal{G} = \mathcal{F}(\lambda)/(eL)$ with $e = 10$ mm the thickness of the plate and $L = 300$ mm its initial length. This takes into account elastic non-linearities in the far-field region ahead of the crack tip. Each plate results in a single $\mathcal{G}(V)$ data point. We have also performed material-saving experiments in which the stretching ratio was increased at a constant rate $\dot{\lambda} = 1.7 \times 10^{-2} \text{ s}^{-1}$. The resulting non-steady crack velocity along the crack path was computed from a piecewise linear fit. We have validated these $\mathcal{G}(V)$ data by comparison with steady-state ones on an overlapping velocity range (Fig. (a)).

Experiments with wetted crack tips are performed by injecting a drop of solvent of about $250\mu\text{l}$ in the tip region while the crack runs. The solvent follows the tip and is prevented from flowing out both thanks to gravity (the crack running down vertically) and capillarity (the solvent wets the gel and forms a meniscus bridging the fracture gap).

* corresponding author: tristan.baumberger@insp.jussieu.fr

¹ Van Vliet, T. & Walstra, P. Large deformation and fracture behaviour of gels. *Faraday Discuss.* **101**, 359–370 (1995).

² Lee, K. Y. & Mooney, D. J. Hydrogels for tissue engineering. *Chem. Rev.* **101**, 1869–1879 (2001).

³ Kong, H. J., Wong, E. & Mooney, D. J. Independent control of rigidity and toughness of polymeric hydrogels. *Macromolecules* **36**, 4582–4588 (2003).

⁴ Mc Evoy, H., Ross-Murphy, S. B. & Clark, A. H. Large deformation and ultimate properties of biopolymer gels: 1. Single biopolymer component systems. *Polymer* **26**, 1483–1492 (1985).

⁵ te Nijenhuis, K. Thermoreversible networks. *Advances in Polymer Science* **130**, Chap. 10 (1997).

⁶ Courty, S., Gornall, J. L. & Terentjev, E. M. Induced helicity in biopolymer networks under stress. *Proc. Nat. Acad. Sci* **102**, 13457–13460 (2005).

⁷ Onuki, A. Theory of phase transition in polymer gels. *Adv. Polymer Sci.* **109**, 63–121 (1993).

⁸ Johnson, D. L. Elastodynamics of gels. *J. Chem. Phys* **77**, 1531–1539 (1982).

- ⁹ Higgs, P. G. & Ross-Murphy, S. B. Creep measurements on gelatin gels. *Int. J. Biol. Macromol.* **12**, 233–240 (1990).
- ¹⁰ Bonn, D., Kellay, H., Prochnow, M., Ben-Djemaa, K., & Meunier, J. Delayed Fracture of an Inhomogeneous Soft Solid. *Science* **280**, 265–267 (1998).
- ¹¹ Lake, G. J. & Thomas, A.G. The strength of highly elastic materials. *Proc. R. Soc. London A* **300**, 108–119 (1967).
- ¹² Nishinari, K., Koide, S. & Ogino, K. On the temperature dependence of elasticity of thermo-reversible gels. *J. Physique* **46**, 793–797 (1985).
- ¹³ Higgs, P. G. & Ball, R. C. Some ideas concerning the elasticity of biopolymer networks. *Macromolecules* **22**, 2432–2437 (1989).
- ¹⁴ Lawn, B. R. Fracture of brittle solids — 2nd edn, Cambridge, University Press (1993).
- ¹⁵ Hui, C.-Y., Jagota, A., Bennison, S. J. & Londono, J. D. Crack blunting and the strength of soft elastic solids. *Proc. R. Soc. London A* **459**, 1489–1516 (2003).
- ¹⁶ Tanaka, T., Hocker, L.O. & Benedek, G. B. Spectrum of light scattered from a viscoelastic gel. *J. Chem. Phys.* **59**, 5151–5159 (1973).
- ¹⁷ Baumberger, T., Caroli, C. & Ronsin, O. Self healing pulses and the friction of gelatin gels. *Eur. Phys. J. E* **11**, 85–93 (2003).
- ¹⁸ Rivlin, R. S. & Thomas, A. G. Rupture of rubber. I. Characteristic energy for tearing. *J. Polymer Sci.* **10**, 291–318 (1953).
- ¹⁹ Laurent, J.-L., Janmey, P. A. & Ferry, J. D. Dynamic viscoelastic properties of gelatin gels in glycerol-water mixtures. *J. Rheol.* **24**, 87–97 (1980).

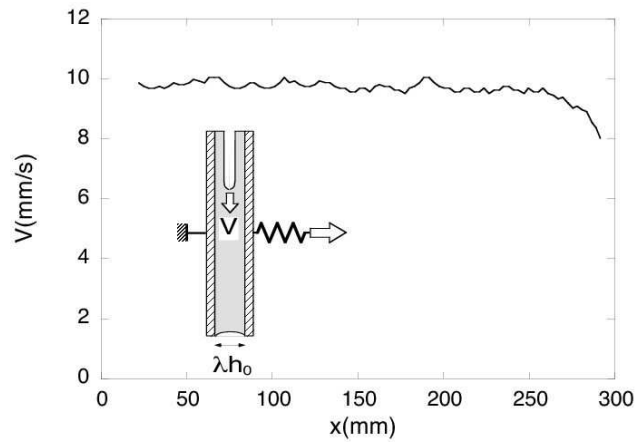
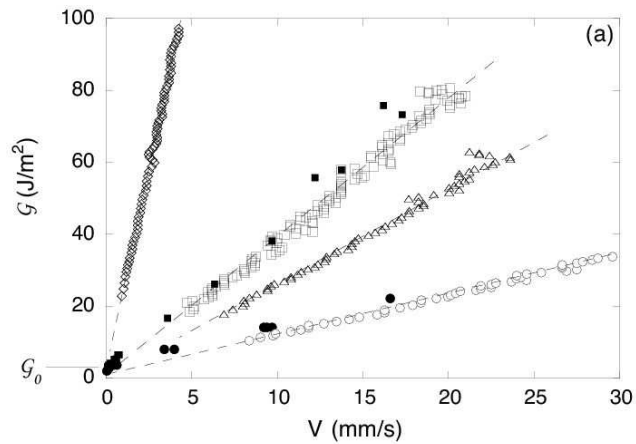


FIG. 1: **Velocity of a stable crack propagating in the mid-plane of a long plate.** Sample: 5 wt % gelatin gel in water, 10 mm thick, 300 mm long, stretched in the transverse direction by a factor $\lambda = 1.3$. The crack was initiated by a single knife-cut notch, 20 mm long. Edge effects extend over about $2h_0$ with $h_0 = 30$ mm the width of the unstretched sample. The remaining central part behaves as a homogeneously stretched plate, hence the observed steady crack-propagation.



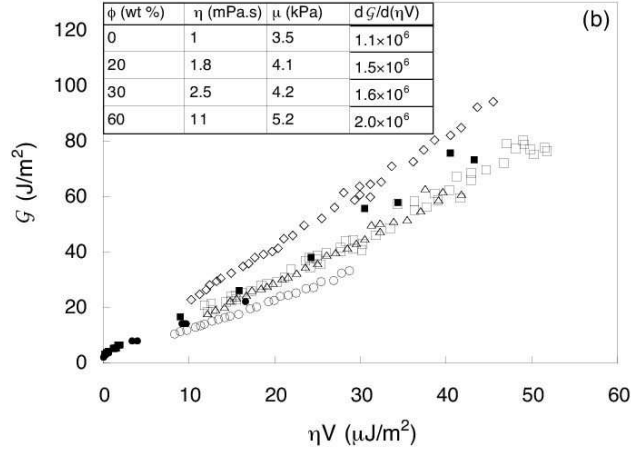


FIG. 2: **Influence of solvent viscosity on the fracture energy $\mathcal{G}(V)$.** **a**, Gels with a constant gelatin content (5 wt %) in water/glycerol solvents with glycerol concentration $\phi = 0$ wt % (circles), 20 wt % (triangles), 30 wt % (squares), 60 wt % (diamonds). Filled symbols correspond to stationary cracks, open symbols to cracks accelerated in response to a steady increase of λ . $\mathcal{G}_0 = 2.5 \pm 0.5 \text{ J.m}^{-2}$ is the common linearly extrapolated toughness. **b**, Plot of \mathcal{G} vs. ηV . Data points have been randomly decimated for clarity. Note the weak systematic growth of $d\mathcal{G}/d(\eta V)$ with glycerol content ϕ elastic modulus μ (see Table).

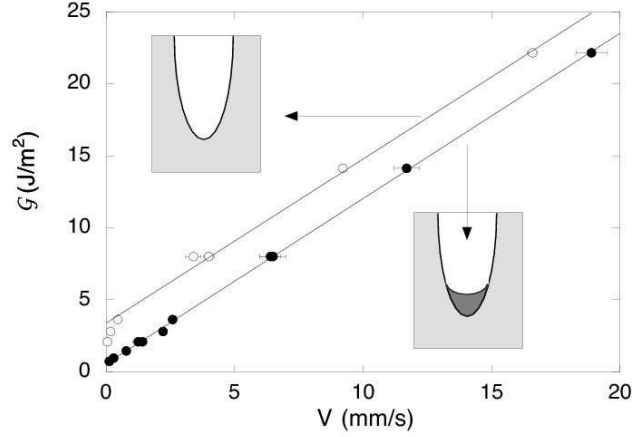


FIG. 3: **Effect of tip homo-wetting.** $\mathcal{G}(V)$ curves for a 5 wt% gelatin gel in pure water : “dry” cracks opening in ambient air (upper data) and “wet” cracks with a drop of pure water soaking the tip. Each pair of points for a given \mathcal{G} corresponds to a single sample. Error bars show standard deviations of velocity along the track. At \mathcal{G} too low for dry cracks to propagate, wet ones can still run. Linear fits are shown. The wet data appear merely translated towards lower energies. The extrapolated fracture energy for wet tips is $\mathcal{G}_0^{wet} = 0.6 \pm 0.15 \text{ J.m}^{-2}$.

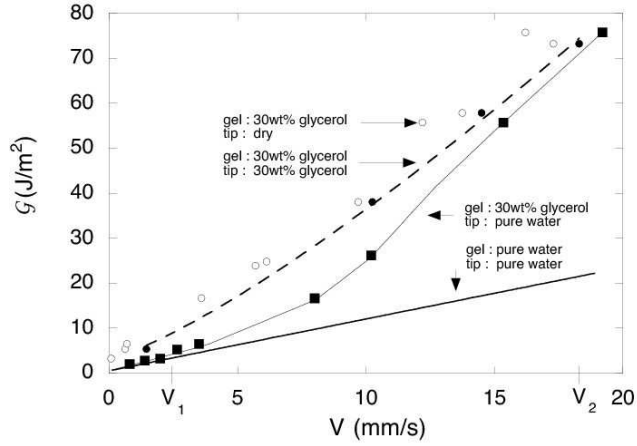


FIG. 4: **Effect of tip hetero-wetting by a less viscous solvent.** The tip of a crack propagating through a gel of gelatin in $\phi = 30\%$ glycerol/water is wetted with pure water (squares). The full curve is a guide for the eye. At low velocities, the data fall on the curve for a gel of gelatin and *pure water* wetted by pure water (full line). At higher velocities ($V_1 \lesssim V \lesssim V_2$), the $\mathcal{G}(V)$ curve crosses over and approaches the one for the glycerolled gel wetted by the same solvent (closed circles and dash line). The data for a $\phi = 30\%$ glycerol/water gel fractured in ambient air (open circles) are shown for comparison.